Eur Radiol (2016) 26:157–166
DOI 10.1007/s00330-015-3817-x

COMPUTED TOMOGRAPHY

Effects of automatic tube potential selection on radiation dose index, image quality, and lesion detectability in pediatric abdominopelvic CT and CTA: a phantom study

Michael F. Brinkley[1] · Juan C. Ramirez-Giraldo[2] · Ehsan Samei[3] · Daniel J. Frush[4] · Kingshuk Roy Choudhury[1] · Joshua M. Wilson[3] · Olav I. Christianson[3] · Donald P. Frush[1]

Received: 15 October 2014 / Revised: 20 April 2015 / Accepted: 21 April 2015 / Published online: 20 May 2015

Abstract
Objectives To assess the effect of automatic tube potential selection (ATPS) on radiation dose, image quality, and lesion detectability in paediatric abdominopelvic CT and CT angiography (CTA).
Methods A paediatric modular phantom with contrast inserts was examined with routine pitch (1.4) and high pitch (3.0) using a standard abdominopelvic protocol with fixed 120 kVp, and ATPS with variable kVp in non-contrast, contrast-enhanced, and CTA mode. The volume CT dose index ($CTDI_{vol}$), contrast-to-noise ratio (CNR) and lesion detectability index (d') were compared between the standard protocol and ATPS examinations.
Results $CTDI_{vol}$ was reduced in all routine pitch ATPS examinations, with dose reductions of 27–52 % in CTA mode ($P<0.0001$), 15–33 % in contrast-enhanced mode ($P=0.0003$) and 8–14 % in non-contrast mode ($P=0.03$). Iodine and soft tissue insert CNR and d' were improved or maintained in all ATPS examinations. kVp and dose were reduced in 25 % of high pitch ATPS examinations and in none of the full phantom examinations obtained after a single full phantom localizer.
Conclusions ATPS reduces radiation dose while maintaining image quality and lesion detectability in routine pitch paediatric abdominopelvic CT and CTA, but technical factors such as pitch and imaging range must be considered to optimize ATPS benefits.
Key Points
- *ATPS automatically individualizes CT scan technique for each patient.*
- *ATPS lowers radiation dose in routine pitch pediatric abdominopelvic CT and CTA.*
- *There is no loss of image quality or lesion detectability with ATPS.*
- *Pitch and scan range impact the effectiveness of ATPS dose reduction.*

Keywords Radiation dosage · Computed tomography · Pediatrics · Radiologic phantom · Radiocontrast agent

Abbreviation

ATPS	Automatic tube potential selection
d'	Lesion detectability index

Introduction

Substantial radiation dose reductions with maintained or improved image quality have been demonstrated with adult contrast-enhanced computed tomography (CT) [1–3] and CT angiography (CTA) [4–9] by lowering CT tube potentials. With smaller cross sectional areas, kVp (kilovoltage peak) reduction has even more potential for dose savings in children

Electronic supplementary material The online version of this article (doi:10.1007/s00330-015-3817-x) contains supplementary material, which is available to authorized users.

✉ Michael F. Brinkley
michael.brinkley@dm.duke.edu

[1] Department of Radiology, Duke University School of Medicine, DUMC Box 3808, Durham, NC 27710, USA

[2] Siemens Healthcare, Malvern, USA

[3] Clinical Imaging Physics Group, Department of Radiology, Duke University School of Medicine, Durham, NC 27710, USA

[4] Medical Physics, Duke University School of Medicine, Durham, NC 27710, USA

as the increased noise from lower kVp is less pronounced in smaller patients and can be compensated for by improved contrast [10–14].

Recent studies have shown a trend towards the use of lower tube potentials in paediatric examinations by manual adjustment of the imaging technique [15]. However, manual adjustments in tube potential can be challenging as they need to account for patient size and examination type at the time of imaging. While reducing tube potential decreases dose and increases iodine contrast, lowering kVp also increases image noise, and hence, an appropriate increase in tube current time product (in milliampere-seconds, mAs) is needed in order to maintain image quality [6, 10, 13].

An automatic tube potential selection tool (ATPS), CARE kV (Siemens Healthcare, Forchheim, Germany), has been recently introduced to facilitate kVp reduction by automatically selecting an optimized combination of tube potential and tube current based on patient body habitus, body part to be imaged, type of examination being performed, and desired image quality [10, 16].

Recent investigations of ATPS addressing adult contrast-enhanced CT and CTA have shown consistent tube potential reduction and radiation dose savings [4, 17–21]. Siegel et al. recently reported a mean 56 % dose reduction in paediatric phantom CTA [22] and a median 27 % dose reduction in paediatric chest and abdominal CT and CTA using ATPS [23]. However, previous studies have been limited with regard to the range of paediatric body sizes investigated and lack of systematic comparison of ATPS results among different examination indication settings. Furthermore, most of these studies have not considered the effects of parameters such as pitch on ATPS, and relied on contrast-to-noise ratio (CNR) as the predominant objective image quality metric.

The purpose of our study was to assess the effects of ATPS on radiation dose, image quality and lesion detectability in paediatric abdominopelvic CT and CTA across a range of paediatric body sizes and examination indications in a phantom. Furthermore, in this study we investigated technique modifications while using ATPS and the resultant impact on dose, image quality and lesion detectability.

Materials and methods

No Institutional Review Board approval was required for this phantom study.

Paediatric phantom A proprietary modular phantom consisting of five different diameter cylindrical sections was used for this investigation (Fig 1a). The four smallest diameter modules of 12 cm, 18.5 cm, 23 cm, and 30 cm, with approximate water equivalent diameters of 11.2 cm, 17.7 cm, 22 cm, and 29 cm, simulating neonate, young child, adolescent, and young adult abdominal diameters, respectively, were used [24]. Each module contained five radially arranged rod inserts, each with a diameter of 25.4 mm and a thickness of 30 mm; the iodine (8.5 mg I/cc) and polystyrene (the soft tissue insert, providing subtle contrast of roughly 50 HU compared to the polyethylene phantom body), were targeted for analysis in this study (Fig 1b).

Automatic tube potential selection (appendix 1) A commercially available tool for ATPS, CARE kV (Siemens Healthcare, Forchheim, Germany), was used for this study. CARE kV automatically selects a combination of tube potential and tube current according to patient size, prescribed image quality, and examination indication. The examination indication is defined with an incremental slider bar with settings 1 to 12, reflecting progressively increased material (i.e., iodine) attenuation from decreasing kVp. In our study, setting 3 was chosen for non-contrast, setting 6 for contrast-enhanced, and setting 9 for CTA examinations (Fig 2).

CT technique All CT images were obtained with spiral technique using the same 128-slice dual source multidetector CT system (Somatom Definition Flash, Siemens Healthcare)

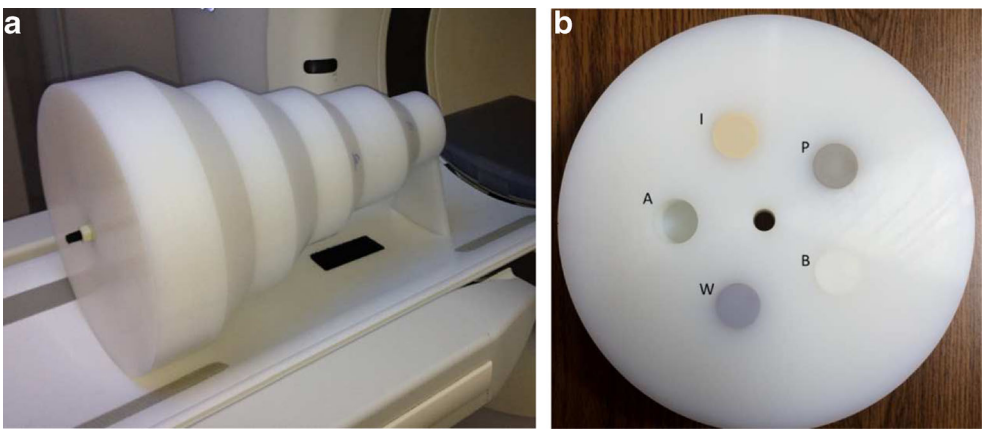

Fig. 1 Photographs of the phantom. The modular phantom (**a**) consists of five different diameter cylindrical modules with intervening tapered sections; the four smallest diameter modules of 12 cm, 18.5 cm, 23 cm, and 30 were used in this study. Each module contains five radially arranged rod inserts (**b**); I = Iodine (8.5 mg I/cc); P = Polystyrene (soft tissue); B = Bone; W = Water; A = Air

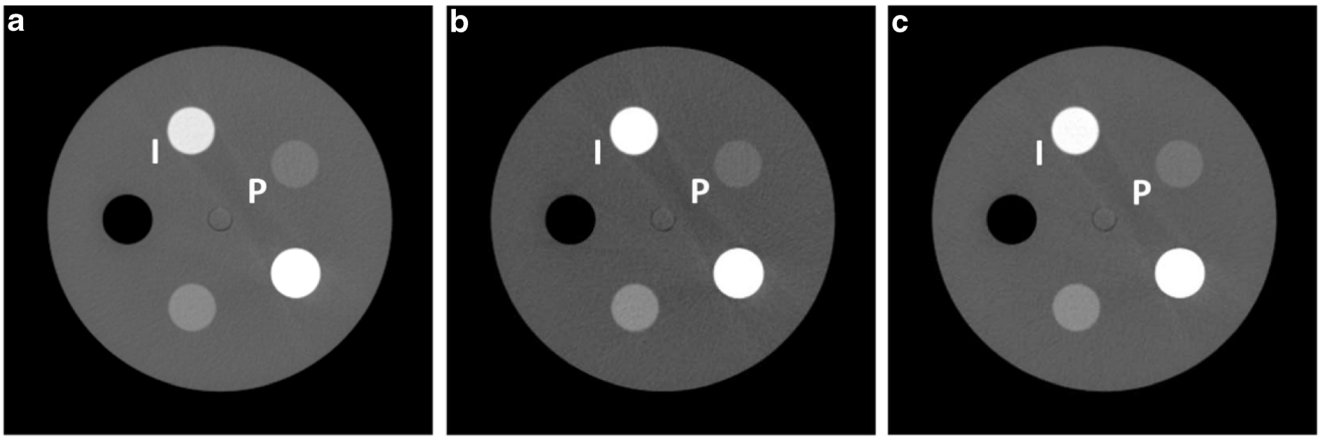

Fig. 2 Axial CT images of the 18.5 cm module demonstrating the impact on iodine (I) and soft tissue (P) inserts scanned (**a**) with standard protocol without ATPS (120 kVp), (**b**) with ATPS in CTA mode (80 kVp chosen by ATPS), and (**c**) with ATPS in non-contrast mode (100 kVp chosen by ATPS). Note that, while noise increased in the lower kVp scans (3.2 in A, 4.3 in B, 3.4 in C), increased iodine insert contrast (311.4 in A, 483.0 in B, 373.3 in C), and to a lesser degree increased soft tissue insert contrast (90.9 in A, 124.1 in B, and 103.7 in C), was demonstrated at lower kVp

equipped with AEC to modulate the tube current (CARE Dose 4D, Siemens Healthcare), ATPS (CARE kV), and Sinogram Affirmed Iterative Reconstruction (SAFIRE) technology. Experimental imaging parameters are provided in Table 1.

Experiment 1. Routine pitch The 12, 18.5, 23, and 30 cm phantom modules were examined independently and identically with a pitch of 1.4, defined as routine pitch, using: 1) routine clinical weight-based paediatric abdominopelvic protocol with a fixed 120 kVp (AEC enabled), and 2) ATPS, with three ATPS examinations performed on each of the four modules (slider bar positions 3, 6, and 9). Each diameter module was examined independently such that the localizer and resultant image adjustments were determined from a single module diameter.

Experiment 2. High pitch Experiment 1 was repeated using a pitch of 3.0 on all scans.

Experiment 3. Full phantom scan All four modules were imaged with a single scan at a pitch of 3.0 using the routine non-ATPS protocol, followed by three ATPS examinations (positions 3, 6 and 9). In these full phantom scans, the resultant scan adjustments were determined based on a localizer of the entire phantom including all four modules, rather than from a localizer of the individual modules.

Radiation Dose and Effective Milliampere Seconds The selected kVp, volume CT dose index ($CTDI_{vol\ 32cm}$), and effective mAs were recorded for each scan. $CTDI_{vol\ 32cm}$ in mGy was used for comparison of delivered radiation dose

Table 1 Experimental imaging parameters

	Experiment 1 – Routine Pitch		Experiment 2 – High Pitch		Experiment 3 – Full Phantom [C]	
	Routine [a]	ATPS[b]	Routine	ATPS	Routine	ATPS
Pitch	1.4	1.4	3.0	3.0	3.0	3.0
Rotation Time (s)	0.5	0.5	0.285	0.285	0.285	0.285
Collimation	128×0.6 mm	128×0.6 mm	128×0.6 mm	128×0.6 mm	128×0.6 mm	128×0.6 mm
Reconstruction	SAFIRE 3	SAFIRE 3	SAFIRE 3	SAFIRE 3	SAFIRE 3	SAFIRE 3
Slice thickness (mm)	5.0	5.0	5.0	5.0	5.0	5.0
Recon interval (mm)	5.0	5.0	5.0	5.0	5.0	5.0
Tube Potential (kVp)	120	variable	120	variable	120	variable
Reference kVp	NA	120	NA	120	NA	120
Reference mAs	200	200	200	200	200	200

[a] Routine = Standard weight-based abdominopelvic pediatric CT protocol with fixed 120 kVp. Automatic Exposure Control (AEC) is enabled

[b] ATPS = Automatic tube potential selection. AEC is enabled

[c] Full Phantom (Experiment 3) = All four diameter modules were included in one continuous scan. In experiments 1 and 2, each diameter module was scanned independently

estimate, and radiation dose subsequently refers to this estimate.

Image Analysis (Appendix 2) Image analysis was performed with a software program developed specifically for the proprietary phantom [25]. Semiautomated measurements and calculations of iodine and soft tissue insert contrast, noise, CNR, and a previously validated detectability index, d', were performed [26]. The detectability index assesses the likelihood of detection of a lesion based on lesion contrast and size (in this study set for the detection of a reference 5 mm lesion, 50 Hounsfield Unit feature contrast), lesion edge profile, system resolution, and noise texture, is a more comprehensive and clinically relevant metric of image quality than CNR alone, and has been demonstrated to correlate with human observer performance [26]. A figure of merit, d'^2 / $CTDI_{vol}$, was further calculated for the iodine and soft tissue inserts to assess lesion detectability per radiation dose.

Statistical analysis The results of the low and high pitch experiments were analyzed independently by fitting a model of the form:

$$\log(Y_{ij}) = \mu + \beta s_j + b_j + \epsilon_{ij}$$

where Y_{ij} is the outcome ($CTDI_{vol}$, d' or CNR) for the i-th module diameter (12, 18.5, 23, 30 cm) and j-th exam setting (routine, ATPS 3, 6, or 9). The model explains the variability in response in terms of the baseline mean μ (which represents the expected response for a phantom of size 12 cm using the routine weight-based protocol and 1.4 pitch), the coefficient of the size term βs_i, and the effect of exam setting b_j. Lastly, ε_{ij} represents measurement error, assumed to have a zero mean Gaussian distribution. The log transform ($\log Y_{ij}$) was used for analysis of d' and CNR to ensure that the response conformed to model assumptions. A $P<0.05$ was considered a significant difference.

Results

Experiment 1. Routine pitch Tube potential was reduced from 120 kVp to either 100 kVp or 80 kVp in all ATPS examinations, with greater tube potential reductions with the smaller phantom diameters and CTA examinations. As expected, average effective mAs increased with all ATPS examinations compared to the routine protocol (Table 2).

Table 2 Experiment 1. Routine Pitch (1.4): Imaging parameter and image quality results of routine protocol with fixed 120 kVp versus automatic tube potential selection protocol

Phantom Diameterr (cm)	Scan Protocol	kVp	$CTDI_{vol}$ (mGy)	% Δ $CTDI_{vol}$	CNR_i	CNR_{st}	d'_i	d'_{st}	$d'^2_i/CTDI_{vol}$	$d'^2_{st}/CTDI_{vol}$
12	Routine	120	5.36	–	165.9	43.2	33.0	33.8	203.1	213.4
	ATPS 3	100	4.63	13.6	192.5	47.5	37.9	37.3	310.1	300.7
	ATPS 6	80	3.6	32.8	233.9	55.0	45.3	41.8	568.8	485.6
	ATPS 9	80	2.55	52.4	196.5	46.2	38.5	35.6	579.9	496.0
18.5	Routine	120	5.99	–	98.8	28.9	19.2	21.8	61.3	79.7
	ATPS 3	100	5.21	13.0	111.3	30.9	21.3	23.4	87.1	105.2
	ATPS 6	100	4.47	25.4	104.3	28.9	20.2	21.8	91.0	106.1
	ATPS 9	80	2.93	51.1	111.2	28.6	21.1	21.4	152.5	156.4
23	Routine	120	6.6	–	62.2	17.9	11.9	13.5	21.5	27.6
	ATPS 3	100	5.91	10.5	73.7	19.8	14.0	14.8	33.2	37.1
	ATPS 6	100	5.22	20.9	68.0	18.2	13.2	14.0	33.6	37.3
	ATPS 9	80	3.54	46.4	73.4	18.6	13.7	13.8	53.2	54.2
30	Routine	120	8.26	–	37.8	11.2	7.2	8.1	6.3	8.0
	ATPS 3	100	7.6	8.0	43.6	12.1	8.3	8.8	9.1	10.1
	ATPS 6	100	7.0	15.3	41.8	11.6	7.8	8.3	8.7	9.9
	ATPS 9	100	6.0	27.4	38.0	10.6	7.2	7.6	8.5	9.6

Routine = Standard weight-based abdominopelvic CT protocol with fixed 120 kVp. Tube current modulation is enabled

ATPS = Automatic tube potential selection. ATPS 3, 6, 9 refer to slider bar positions 3, 6, 9 on the CARE kV user interface

%Δ $CTDI_{vol}$=% reduction in $CTDI_{vol}$ with ATPS compared to the routine examination of the same phantom diameter

CNR_i and CNR_{st} = contrast to noise ratio for the iodine and soft tissue inserts

d'_i and d'_{st} = detectability index of the iodine (i) and soft tissue (st) inserts

* Full data set (including avg mAs_{eff}, contrast and noise values) and statistical analysis available in online supplementary material

The reduction in kVp was accompanied by a reduction in $CTDI_{vol}$ in all ATPS examinations, with progressive dose reduction in non-contrast, contrast-enhanced, and CTA examinations (Fig. 3). Dose reductions ranged from 27.4–52.4 % in the CTA mode ($P<0.0001$), 15.3–32.8 % in the contrast enhanced mode ($P=0.0003$), and 8.0–13.6 % in the non-contrast mode ($P=0.03$), with the greatest dose reductions in the smaller phantom diameters for each examination type (Table 2; statistical analysis results available in online supplementary material).

Metrics of image quality were either improved or maintained with ATPS. There was a statistically significant increase in CNR_{iodine} for non-contrast and contrast-enhanced ATPS examinations ($P=0.019$ and $P=0.017$, respectively), and a statistically significant increase in d'_{iodine} for non-contrast and contrast-enhanced ATPS examinations ($P=0.019$ and $P=0.018$, respectively). Increases in $CNR_{soft\ tissue}$ and $d'_{soft\ tissue}$ in 83 % and 75 % of ATPS exams, respectively, did not achieve statistical significance (Table 2).

The figures of merit d'^2_{iodine} / $CTDI_{vol}$ and $d'^2_{soft\ tissue}$ / $CTDI_{vol}$ were increased in all ATPS examinations, consistent with better image quality per dose (Fig. 4a, b).

Our analysis also allows for an assessment of the overall effect of phantom diameter on dose and image quality, with a statistically significant increase in $CTDI_{vol}$ ($P<0.0001$) and a statistically significant decrease in image quality ($P<0.0001$ for $d'_{iodine\ and\ soft\ tissue}$ and $CNR_{iodine\ and\ soft\ tissue}$) with increasing phantom size (Table 2).

Experiment 2. High pitch With the high pitch (3.0) protocol, there was more limited kVp reduction with ATPS, with selection of a reduced kVp (100 kVp) in only 3/12 (25 %) ATPS examinations (Table 3). Dose reductions of 31.1–35.2 % were observed in these three lower kVp examinations (Fig. 5), but an overall statistically significant dose reduction was not achieved given the lack of kVp reduction in the remaining examinations (Table 3; statistical analysis results available in online supplementary material). In the 9/12 ATPS examinations without kVp reduction, both the selected kVp and effective mAs were essentially unchanged from the routine protocol, thus there were no differences in radiation dose (Fig. 5).

While the ATPS examinations performed at 100 kVp did demonstrate a trend towards improved CNR_{iodine}, d'_{iodine}, d'^2_{iodine} / $CTDI_{vol}$ and $d'^2_{soft\ tissue}$ / $CTDI_{vol}$, overall image quality was maintained but not improved, with no statistically significant difference in $d'_{iodine\ or\ soft\ tissue}$ and $CNR_{iodine\ or\ soft\ tissue}$ between the ATPS and routine protocol examinations (Table 3).

Experiment 3. Full phantom ATPS did not reduce tube voltage in the full phantom scans. Without a kVp reduction, there was effectively no difference in effective mAs, dose, image noise, insert contrast, or lesion detectability between the ATPS and routine protocol examinations (Table 4).

Discussion

Our results demonstrate that ATPS technology can be an effective tool to reduce radiation dose while maintaining or improving image quality in paediatric abdominopelvic CT and CTA. However, the way in which this technology is used can impact dose reduction and image quality. The results of our

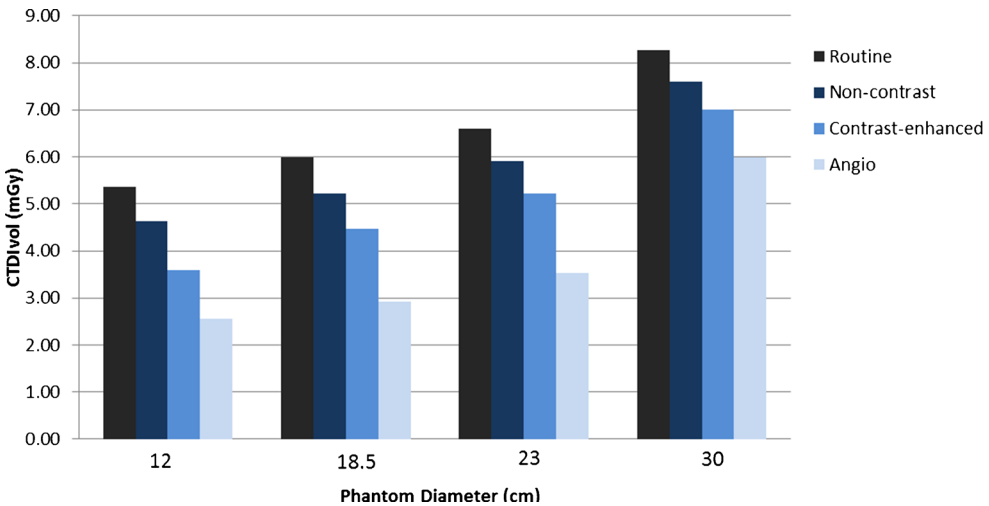

Fig. 3 Routine Pitch (1.4). Bar graph of radiation exposure, as measured by the volume CT dose index ($CTDI_{vol}$), relative to examination type for each of the four module diameters using routine (weight-based abdominopelvic pediatric CT protocol with fixed 120 kVp) and ATPS (with variable kVp) protocols. Non-contrast, contrast-enhanced, and angio refer to ATPS exams at slider bar positions 3, 6, and 9, respectively, on the CARE kV interface. Dose reductions were observed with all ATPS examinations (14–52 % reductions with 12 cm module, 13–51 % reductions with 18.5 cm module, 11–46 % reductions with 23 cm module, and 8–27 % reductions with 30 cm module), with the largest dose reductions observed with the smaller modules and angio mode

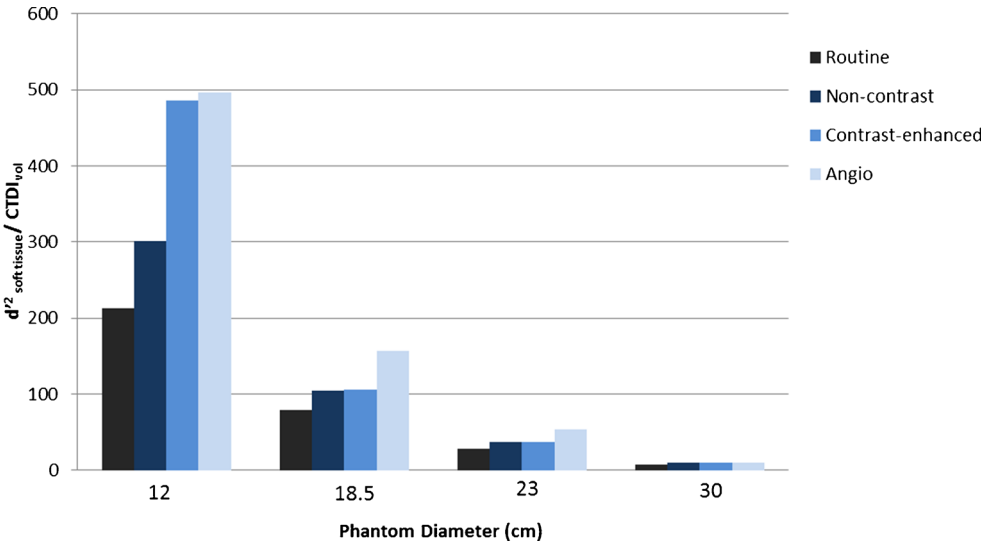

Fig. 4 Figure of Merit. Bar graph of the figure of merit for the (**a**) iodine insert (d'^2_{iodine} / $CTDI_{vol}$) and (**b**) soft tissue insert ($d'^2_{soft\ tissue}$ / $CTDI_{vol}$) in the routine pitch experiment. At each module diameter, lesion detectability per unit of radiation dose (mGy) was increased with all ATPS examinations compared to the routine protocol. Non-contrast, contrast-enhanced, and angio refer to ATPS exams at slider bar positions 3, 6, and 9, respectively

routine pitch experiment are in agreement with previous ATPS phantom studies demonstrating the greatest dose reductions with CTA exams and smaller phantom sizes [4, 22]. The 52.4 %, 51.1 %, and 46.4 % dose reductions with the CTA examinations in the 12 cm, 18.5 cm, and 23 cm modules are similar to recently published results of a mean 56 % dose reduction in paediatric phantom CTA [22]. These findings have important clinical implications regarding potential cancer risks in young patients given the generally recognized increased susceptibility of the youngest, smallest children [27–30]. Moreover, while not tested in prior investigations, we also found substantial dose

Table 3 Experiment 2. High Pitch (3.0): Imaging parameter and image quality results of routine protocol with fixed 120 kVp versus automatic tube potential selection protocol examinations

Phantom Diameter (cm)	Scan Protocol	kVp	$CTDI_{vol}$ (mGy)	% Δ $CTDI_{vol}$	CNR_i	CNR_{st}	d'_i	d'_{st}	$d'^2_i/CTDI_{vol}$	$d'^2_{st}/CTDI_{vol}$
12	Routine	120	5.46	–	143.5	36.2	29.1	30.4	155.3	169.4
	ATPS 3	120	5.46	0.0	143.4	38.3	29.0	32.2	153.9	190.3
	ATPS 6	100	3.76	31.1	151.5	39.3	30.4	31.9	146.3	269.8
	ATPS 9	100	3.54	35.2	149.9	36.5	30.3	30.1	259.8	255.6
18.5	Routine	120	5.79	–	95.9	28.5	18.1	21.6	56.4	80.9
	ATPS 3	120	5.83	0.0	93.0	27.4	18.2	21.9	57.1	82.0
	ATPS 6	120	5.81	0.0	94.5	26.8	17.9	21.0	55.2	76.0
	ATPS 9	100	3.76	35.1	96.7	25.4	18.6	20.2	91.7	108.2
23	Routine	120	6.62	–	64.2	18.4	11.7	13.9	20.7	29.1
	ATPS 3	120	6.62	0.0	63.1	17.8	11.7	13.6	20.7	27.8
	ATPS 6	120	6.63	0.0	63.7	17.7	11.8	13.6	21.1	28.0
	ATPS 9	120	6.62	0.0	63.3	17.8	12.0	13.8	21.6	28.6
30	Routine	120	7.67	–	38.2	11.4	6.9	8.1	6.2	8.5
	ATPS 3	120	7.68	0.0	39.1	11.4	7.3	8.5	7.0	9.5
	ATPS 6	120	7.68	0.0	38.4	10.6	7.2	7.9	6.7	8.1
	ATPS 9	120	7.68	0.0	38.5	11.3	7.0	8.1	6.4	8.5

Routine = Standard weight-based abdominopelvic CT protocol with fixed 120 kVp. Tube current modulation is enabled

ATPS = Automatic tube potential selection. ATPS 3, 6, 9 refer to slider bar positions 3, 6, 9 on the CARE kV user interface

%Δ $CTDI_{vol}$ = % reduction in $CTDI_{vol}$ with ATPS compared to the routine examination of the same phantom diameter

CNR_i and CNR_{st} = contrast to noise ratio for the iodine and soft tissue inserts

d'_i and d'_{st} = detectability index of the iodine (i) and soft tissue (st) inserts

* Full data set (including avg mAs_{eff}, contrast and noise values) and statistical analysis available in online supplementary material

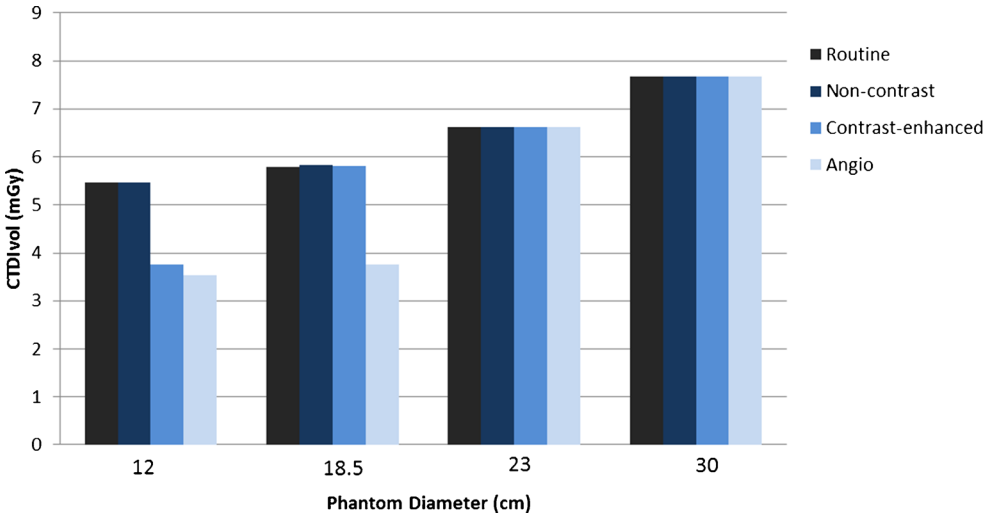

Fig. 5 High Pitch (3.0). Bar graph of radiation exposure, as measured by the volume CT dose index ($CTDI_{vol}$), relative to examination type for each of the four module diameters using routine (weight-based abdominopelvic paediatric CT protocol with fixed 120 kVp) and automatic tube potential selection (with variable kVp) protocols. Non-contrast, contrast-enhanced, and angio refer to ATPS examinations at slider bar positions 3, 6, and 9, respectively, on the CARE kV interface. Dose reductions were observed in only 25 % of the high pitch scans, with dose reductions with the 12 cm module (31 % in contrast-enhanced mode and 35 % in angio mode) and the 18.5 cm module (35 % in angio mode)

reductions with the larger phantom diameters and with the contrast-enhanced and non-contrast-enhanced ATPS scans, supporting ATPS applicability to a range of paediatric body sizes and clinical indications.

To our knowledge, this is the first systematic study of ATPS across a range of paediatric sizes and selected examination indications (non-contrast, contrast-enhanced, and angiography). This study provides a more comprehensive and clinically relevant assessment of image quality, as the detectability index, in addition to the standard CNR, was measured and compared for both the iodine and soft tissue inserts. We chose to evaluate both inserts on all scans, thereby assessing the effect of the CTA setting not only on the iodine insert, but also on soft tissue contrast and lesion detectability, and vice versa. We feel this approach affords an expanded and more clinically appropriate image quality analysis. In addition to maintaining or improving CNR for the iodine and soft tissue inserts in all ATPS scans, figures of merit $d'^2/ CTDI_{vol}$ were also increased in all ATPS scans, consistent with improved lesion detectability per radiation dose.

In experiment 2 we examined variations on pitch for ATPS. In 75 % of the high pitch ATPS examinations, there was no kVp reduction and, hence, no dose savings, likely a result of limitations in tube power for the high pitch scans. Lowering the kVp typically requires an increase in mAs in order to maintain the desired CNR, and when the existing x-ray tube generator is unable to achieve the necessary mAs, ATPS automatically selects the next highest kVp that can provide the

Table 4 Experiment 3. Full Phantom: Imaging parameter and image quality results of routine protocol with fixed 120 kVp versus automatic tube potential selection protocol examinations

Phantom Diameter (cm)	kVp	$CTDI_{vol}$	CNR_i	CNR_{st}	d'_i	d'_{st}	$d'^2_i/CTDI_{vol}$	$d'^2_{st}/CTDI_{vol}$
Routine	120	6.44	94.09	26.81	17.4	20.6	47.2	65.6
ATPS 3	120	6.43	95.47	27.74	18.1	21.8	50.8	73.8
ATPS 6	120	6.44	94.33	26.86	17.4	20.5	46.8	65.2
ATPS 9	120	6.44	96.55	27.27	18.0	21.2	50.1	70.0

Routine = Standard weight-based abdominopelvic CT protocol with fixed 120 kVp. Tube current modulation is enabled

ATPS = Automatic tube potential selection. ATPS 3, 6, 9 refer to slider bar positions 3, 6, 9 on the CARE kV user interface

%Δ $CTDI_{vol}$=% reduction in $CTDI_{vol}$ with ATPS compared to the routine examination of the same phantom diameter

CNR_i and CNR_{st} = contrast to noise ratio for the iodine and soft tissue inserts

d'_i and d'_{st} = detectability index of the iodine (i) and soft tissue (st) inserts

* Full data set (including avg mAs_{eff}, contrast and noise values) and statistical analysis available in online supplementary material

desired image quality. In the high pitch, dual source scan, the maximum effective mAs that the system can reach is limited by a faster rotation time and higher pitch, and thus may not be able to achieve the increased mAs required to examine at a lower kVp. Schindera et al., demonstrated the limitations of maximum tube current on automatic tube potential reduction by using a progressively smaller pitch value in order to perform a lower kVp examination [4]. While increasing pitch is often considered a means for dose reduction, use of a higher pitch may restrict the ability of ATPS to lower kVp and thus may limit ATPS dose savings in certain situations. Application of the results of this investigation can help guide examination performance using ATPS based on patient size, region scanned, and indication. For example, high pitch thoracic CTA in an infant using ATPS may allow for kVp and dose reductions given the small patient size, improved iodine contrast at lower kVp, and the lower effective mAs in thoracic imaging. However, in an older and larger child, the high pitch mode may preclude full realization of ATPS image quality and dose benefits due to tube current limits; using a lower pitch with ATPS may allow for kVp and resultant dose reductions.

The lack of tube voltage adaptation with the full phantom examinations following a full phantom topogram (experiment 3) indicates that the ability of ATPS to reduce kVp is limited with combination CT exams covering multiple body regions of variable diameters where the thickest sections will determine kVp for the entire scan thus limiting kVp reduction. Similar to experiment 2, tube current limitations likely prevented the use of a lower kVp due to insufficient tube power reserve; hence, the reference tube potential (120 kVp) was unchanged and exposure adaptation was due solely to the AEC. Our results stress the importance of limiting the scan area to the region of interest in addition to considering split versus combination examinations in order to maximize kVp reduction. For example, including the neck and chest in a single scan would be a suboptimal use of ATPS technology as kVp adaptation would be biased towards using a higher kVp due to the larger attenuation of the shoulder region.

Our study has limitations that warrant consideration. First, this a phantom study, so actual z-axis and angular variations in patient thickness and organ attenuation that may affect tube potential and tube current modulation would not be accounted for in this study. Second, the experiments were performed on a single CT scanner using a specific manufacturer's proprietary automatic tube potential selection technology. Third, estimated $CTDI_{vol}$ was used for comparison of radiation dose. While we demonstrate ATPS reductions in $CTDI_{vol}$, a measure of scanner output that should translate into decreased radiation dose to the patient, we did not evaluate estimated patient effective dose or actual dose to the phantom. The use of $CTDI_{vol\ 32\ cm}$ (as opposed to $CTDI_{vol\ 16\ cm}$) would underestimate the absolute value of the radiation exposure for the smaller phantom diameters, but percent dose reductions, which were the focus in this study, would remain unchanged. Fourth, we did not perform a qualitative observer evaluation of image quality. However, a strength of our study is the more comprehensive quantitative evaluation of image quality using both CNR and lesion detectability, which would translate to perceptual changes; recent ATPS studies have shown maintenance of diagnostic quality images at reduced kVp [17–21, 23]. Fifth, we selected 120 kVp as the routine protocol kVp and ATPS reference kVp for all examinations. In many institutions, routine weight-based protocols would call for a kVp of less than 120 in smaller paediatric patients [15], but since we were imaging and comparing a range of phantom diameters (including a young adult equivalent) we elected to use 120 kVp. Finally, our selections of positions 3, 6, and 9 to represent non-contrast, contrast-enhanced, and CTA examinations, respectively, differ slightly from the default labels provided on the CARE kV interface (where 3 = non-contrast, 7 = contrast-enhanced liver, and 11 = CTA). The slider bar selection reflects a trade-off between iodine contrast gain and image noise, and our selection of position 9 for CTA reflects a preference for a lower noise CTA examination in our actual practice. Selecting a higher contrast gain (slider bar position >9) would weight the examination towards improved iodine contrast, lower kVp, and potentially more dose savings.

ATPS can reduce radiation dose and maintain image quality across a range of paediatric abdominopelvic examination indications and body sizes, and, where available, this technology can be easily implemented into everyday clinical practice. Using ATPS, dose reductions can be achieved from already low dose protocols and even greater dose reductions are anticipated in the non-paediatric hospital setting.

Acknowledgements The scientific guarantor of this publication is Donald P. Frush. The authors of this manuscript declare relationships with the following companies: Juan C. Ramirez-Giraldo is an employee of Siemens Healthcare. Ehsan Samei has research grants from GE and Siemens. The authors state that this work has not received any funding. One of the authors has significant statistical expertise: Kingshuk Roy Choudhury. Institutional Review Board approval was not required because this is a phantom study. Methodology: prospective, experimental, performed at one institution.

Appendix 1 Automatic Tube Potential Selection (ATPS) (CARE kV, Siemens Healthcare)

CARE kV is a commercially available ATPS software tool which automatically selects a combination of tube potential and tube current according to patient size, prescribed image quality, and examination indication. The patient size is estimated by the use of the CT radiograph localizer (topogram). To define the examination indication and to prescribe the reference image quality, the CARE kV tool uses three parameters: the quality reference mAs, the reference kVp, and the

examination type. The quality reference mAs is needed by the automated exposure control system (CARE Dose 4D, Siemens Healthcare). The reference kVp is to be set according to an institution's established routine clinical protocols, which in conjunction with the defined quality reference mAs are known to provide consistent image quality for a reference patient weighting 70 kg. The examination indication is defined with an incremental slider bar with settings 1 to 12. Lower settings (1–4) are best suited for non-contrast examinations where CARE kV expects the user will accept little or no increase in image noise. Mid-range settings (5–8) are best suited for contrast-enhanced examinations where CARE kV assumes the user will accept a small increase in image noise that will be balanced by a boost of iodine contrast when a lower kVp is selected. Higher settings (9–12) are best suited for CTA examinations where the user expects gains in iodine contrast at lower kVp to offset increased image noise at the lower kVp values. CARE kV aims to maintain the desired CNR as defined by the reference kVp and quality reference mAs.

Appendix 2 Image Analysis with IMQUEST analysis software

Image analysis software developed specifically for the proprietary phantom was used for image analysis. Square ROIs were drawn by a single investigator (40 mm side length for contrast evaluation and 50 mm side length for noise evaluation) with semiautomated measurement of image contrast (contrast = HU_{insert} - $HU_{polytethylene\ body}$) and image noise (noise = pixel standard deviation of ROIs placed within the uniform phantom body). Contrast-to-noise ratios (CNR = $contrast_{insert}$ / noise) were calculated for the iodine and soft tissue inserts. A previously validated lesion detectability index, d', for the iodine and soft tissue inserts was calculated, presented in a simplified format:

$$d'^2 = \left(\iint W^2 \cdot TTF^2 \cdot E^2\right)^2 \Big/ \left(\iint W^2 \cdot TTF^2 \cdot E^4 \cdot NPS\right)$$

where W is the task function, set for the detection of a reference 5 mm designer nodule [31]; TTF is the task transfer function, a measure of system resolution as a function of spatial frequency; E is the Eye Filter, reflecting human visual response characteristics at a typical 60 cm viewing distance; and NPS is the noise power spectrum, a measure of the magnitude and texture characteristics of noise. The d' values were adjusted to represent a reference feature contrast of 50 Hounsfield Units at 120 kVp for the 12 cm phantom.

References

1. Funama Y, Awai K, Nakayama Y et al (2005) Radiation dose reduction without degradation of low-contrast detectability at abdominal multisection CT with a low-tube voltage technique: phantom study. Radiology 237(3):905–910
2. Nakayama Y, Awai K, Funama Y et al (2005) Abdominal CT with low tube voltage: preliminary observations about radiation dose, contrast enhancement, image quality, and noise. Radiology 237(3):945–951
3. Marin D, Nelson RC, Schindera ST et al (2010) Low-tube-voltage, high-tube-current multidetector abdominal CT: improved image quality and decreased radiation dose with adaptive statistical iterative reconstruction algorithm – initial clinical experience. Radiology 254(1):145–153
4. Schindera ST, Winklehner A, Alkadhi H, et al (2013) Effect of automatic tube voltage selection on image quality and radiation dose in abdominal CT angiography of various body sizes: a phantom study. Clin Radiol 68(2): e79-86. http://www.sciencedirect.com/science/article/pii/S0009926012005259. Accessed January 17, 2014
5. Kalva SP, Sahani DV, Hahn PF, Saini S (2006) Using the K-edge to improve contrast conspicuity and to lower radiation dose with a 16-MDCT: a phantom and human study. J Comput Assist Tomogr 30(3):391–397
6. Yu L, Li H, Fletcher JG, McCollough CH (2010) Automatic selection of tube potential for radiation dose reduction in CT: a general strategy. Med Phys 37(1):234–243
7. Kalender WA, Deak P, Kellermeier M, van Straten M, Vollmar SV (2009) Application- and patient size-dependent optimization of x-ray spectra for CT. Med Phys 36(3):993–1007
8. Bischoff B, Hein F, Meyer T et al (2009) Impact of a Reduced Tube Voltage on CT Angiography and Radiation Dose: Results of the Protection 1 Study. JACC Cardiovasc Imaging 2(8):940–946
9. Nakayama Y, Awai K, Funama Y et al (2006) Lower tube voltage reduces contrast material and radiation doses on 16-MDCT aortography. AJR 187(5):W490–W497
10. Raman S, Johnson P, Deshmukh S, Mahesh M, Grant KL, Fishman EK (2013) CT dose reduction applications: available tools on the latest generation of CT scanners. J Am Coll Radiol 10(1):37–41
11. Young C, Owens C (2013) Pediatric computed tomography imaging guideline. Acta Radiol 54(9):998–1006
12. Siegel MJ, Schmidt B, Bradley D, Suess C, Hildebolt C (2004) Radiation dose and image quality in pediatric CT: effect of technical factors and phantom size and shape. Radiology 233(2):515–522
13. Yu L, Liu X, Leng S et al (2009) Radiation dose reduction in computed tomography: techniques and future perspective. Imaging Med 1(1):65–84
14. Yu L, Bruesewitz MR, Thomas KB, Fletcher JG et al (2011) Optimal tube potential for radiation dose reduction in pediatric CT: principles, clinical implementations, and pitfalls. Radiographics 31(3):835–848
15. Arch ME, Frush DP (2008) Pediatric body MDCT: a 5-year follow-up survey of scanning parameters used by pediatric radiologists. AJR 191(2):611–617
16. Grant K, Schmidt B (2011) CARE kV: Automated Dose-Optimized Selection of X-ray Tube Voltage, White Paper
17. Goetti R, Winklehner A, Gordic S et al (2012) Automated attenuation-based kilovoltage selection: preliminary observations in patients after endovascular aneurysm repair of the abdominal aorta. AJR 199(3):W380–W385
18. Hough DM, Fletcher JG, Grant KL et al (2012) Lowering kilovoltage to reduce radiation dose in contrast-enhanced abdominal CT: Initial assessment of a prototype automated kilovoltage selection tool. AJR 199(5):1070–1077
19. Eller A, May MS, Scharf M et al (2012) Attenuation-based automatic kilovolt selection in abdominal computed tomography: effects of radiation exposure and image quality. Invest Rad 47(10): 559–565

20. Lee KH, Lee JM, Moon SK et al (2012) Attenuation-based automatic tube voltage selection and tube current modification for dose reduction at contrast-enhanced liver CT. Radiology 265(2):437–447
21. Mayer C et al (2014) Potential for radiation dose savings in abdominal and chest CT using automatic tube voltage selection in combination with automatic tube current modulation. AJR 203:292–299
22. Siegel MJ, Ramirez-Giraldo JC, Hildebolt C, Bradley D, Schmidt B (2013) Automated low- kilovoltage selection in pediatric computed tomography angiography. Phantom study evaluating effects on radiation dose and image quality. Invest Radiol 48(8):584–589
23. Siegel MJ, Hildebolt C, Bradley D (2013) Effects of automated kilovoltage selection technology on contrast-enhanced pediatric CT and CT angiography. Radiology 268(2):538–547
24. Kleinman PL, Strauss KJ, Zurakowski D, Buckley KS, Taylor GA (2010) Patient size measured on CT images as a function of age at a tertiary care children's hospital. AJR 194(6):1611–1619
25. Wilson JM, Christianson OI, Richard S, Samei E (2013) A methodology for image quality evaluation of advanced CT systems. Med Phys 40(3):031908
26. Gang GJ, Lee J, Stayman JW et al (2011) Analysis of Fourier-domain task-based detectability index in tomosynthesis and cone-beam CT in relation to human observer performance. Med Phys 38(4):1754–1768
27. Brenner DJ, Hall EJ (2007) Computed tomography – an increasing source of radiation exposure. N Engl J Med 357(22):2277–2284
28. Brody AS, Frush DP, Huda W, Brent RL (2007) Radiation risk to children from computed tomography. Pediatrics 120(3):677–682
29. National Academies (2006) Biologic Effects of Ionizing Radiation (BEIR) Report VII: Health risks from exposure to low levels of ionizing radiation
30. Journy N, Ancelet S, Rehel JL, et al (2013) Predicted cancer risk induced by computed tomography examinations during childhood, by a quantitative risk assessment approach. Radiat Environ Biophys; epub. http://link.springer.com/article/10.1007%Fs00411-013-0491-8/fulltext.html. Accessed January 17, 2014
31. Samei E, Flynn MJ, Eyler WR (1997) Simulation of subtle lung nodules in projection chest radiography. Radiology 202(1): 117–124